

Journal of Biomedical Optics

SPIEDigitalLibrary.org/jbo

Assessment of interfacial defects at composite restorations by swept source optical coherence tomography

Kyung-Jin Park
Hartmut Schneider
Rainer Haak

Assessment of interfacial defects at composite restorations by swept source optical coherence tomography

Kyung-Jin Park, Hartmut Schneider, and Rainer Haak

University of Leipzig, Department of Cariology, Endodontology and Periodontology, Liebig Street 12, Haus 1, 04103 Leipzig, Germany

Abstract. In clinical dental practice, it is often difficult or even impossible to detect and assess interfacial adhesive defects at adhesive restorations by means of visual inspection or other established diagnostic methods. However, nondestructive optical coherence tomography (OCT) may provide a better picture in this diagnostic scenario. The aim of this study was to evaluate the suitability of swept source OCT (SS-OCT) for the nondestructive assessment of interfacial deficiencies at composite restorations and the evaluation of cohesive defects within composite material. Ten class V composite restorations that were not adhesively luted were taken as validation objects and examined for frequency of interfacial gaps, air entrapments, and defects between composite layers using SS-OCT with a 1325-nm center wavelength. Light microscopy was used to inspect for inherent structures. SS-OCT detected $79.5\% \pm 1.8\%$ of the total gap lengths at the enamel interface and $70.9\% \pm 0.4\%$ at the dentin interface. Additionally, defective structures in composite restorations were displayed. It was shown that OCT imaging has the potential to nondestructively assess the interfacial adaptation of composite restorations and to detect internal defects in the layered composite material. © The Authors. Published by SPIE under a Creative Commons Attribution 3.0 Unported License. Distribution or reproduction of this work in whole or in part requires full attribution of the original publication, including its DOI. [DOI: [10.1117/1.JBO.18.7.076018](https://doi.org/10.1117/1.JBO.18.7.076018)]

Keywords: optical coherence tomography; swept source optical coherence tomography; interfacial adhesive defects; composite restoration; diagnostics.

Paper 130215R received Apr. 6, 2013; revised manuscript received Jun. 17, 2013; accepted for publication Jul. 2, 2013; published online Jul. 22, 2013.

1 Introduction

In clinical dental practice, adhesive defects between tooth substance and composite (Composite: type of synthetic resins which is used in dentistry as adhesives.) restorations [interfacial (Interface: boundary between adjacent substances or phases.) defects], which adversely affect restoration quality, cannot be avoided due to polymerization shrinkage, different thermal expansion of tooth substance and composite, and composite degradation.¹ A longitudinal assessment of this interface would therefore be beneficial for revealing degradation effects in the bonding interface over time. During mastication, saliva and other liquids may enter the gaps under pressure, resulting in detachment of the adhesive interface, or deformation of restoration margins.² This in turn may allow further penetration of saliva and microorganisms into the tooth—composite interface, bringing discoloration, hypersensitivity, plaque accumulation, and may potentially lead to the development of a caries lesion, which is the main reason for composite restorations to be replaced.³ However, this costly procedure can be delayed as long as possible with early detection and monitoring of gap or defect progression adjacent to restorations. The detection and assessment of interfacial gaps together with longitudinal monitoring of gap progression are therefore of great clinical significance. However, it is difficult to visually detect or assess gaps at the tooth—composite interface before large defects occur. Another important focus of assessment is to differentiate between merely discolored gaps⁴ on the one hand and defects with additional active carious damage on the other.

Radiography is the most frequently used supplementary diagnostic technique, but it offers limited information about

marginal discrepancies or gaps in adhesively luted composite restorations. It has been reported that the radiographic marginal gap detection frequently results in false positive or false negative results,⁵ which can lead to unnecessary intervention or under-treatment. Micro-computer tomography addresses these issues *in vitro*, as it has the disadvantage of exposing the specimen to high radiation hazards and therefore, is far from ready for clinical application. New noninvasive imaging methods enabling surface and subsurface assessment of composite restorations are therefore desirable.

Optical coherence tomography (OCT) is an imaging method using low coherence interferometry. The principle upon which it is based has already been described in numerous publications.^{6–9} Light is split into two arms—a sample arm (at the end of which lies the observed object) and a reference arm. The interference of scattered/reflected light from the sample arm and reference arm gives rise to an interference pattern.^{6,10} This tomographic method allows contact-free nondestructive real time imaging with high, micron-scale resolution by analyzing the echo time delay, and intensity of light backscattered by internal microstructures in objects. In addition, the method generates data sets for three-dimensional volumetric images without high-risk radiation, making it suitable for *in vivo* applications.

The aim of this study was to evaluate the suitability of swept source OCT (SS-OCT) at a 1325-nm center wavelength to nondestructively assess interfacial adhesive defects in terms of size and frequency and to characterize defective structures in composite restorations. The study prepared specimens with an adhesive defect at the tooth—composite interface as validation objects, and hypothesizes that SS-OCT is suitable for detecting and assessing adhesive defects at the composite—tooth interface and for imaging morphological details inside composite restorations up to a depth of 3.0 mm.

Address all correspondence to: Kyung-Jin Park, University of Leipzig, Department of Cariology, Endodontology and Periodontology, Liebig Street 12, Haus 1, 04103 Leipzig, Germany. Tel: +49-341-97-21212; Fax: +49-341-97-21219; E-mail: kyungjin.park@medizin.uni-leipzig.de

2 Materials and Methods

2.1 Preparation of Specimens

Ten intact, extracted caries-free human molars were selected and immersed in 0.5% chloramine solution at 4°C immediately after extraction. The teeth were cleaned mechanically. Standardized, box-shaped class V cavities (Class V cavities: cavities on the junction of the crown and root.) with dimensions of 3 mm coronal-apically, 4 mm mesio-distally, and 1.5 mm in depth in average were prepared with a rounded cylindrical diamond bur (107 μm , 836 KR 314014, Komet®/Gebr. Brasseler, Lemgo, Germany) (Fig. 1). The cavities were placed at the vestibular cement–enamel junction in order to provide an equally extended cavity margin at crown (enamel) and root (dentine). The cavity

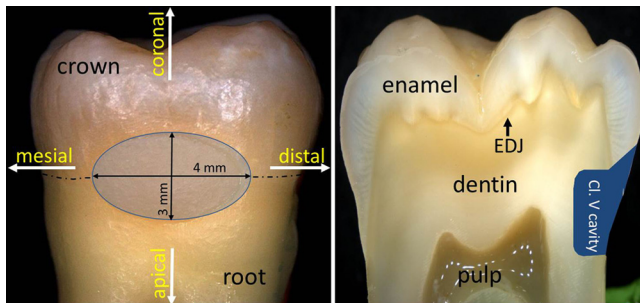


Fig. 1 General overview of specimen showing position and extent of class V cavity. (a) Frontal view and (b) cross sectional view. Class V cavity marked in blue. Class V cavity was prepared at the junction between crown and root (dotted line) measuring $4 \times 3 \text{ mm}^2$ (1.5 mm in depth). Also shown are tooth cardinal directions: “apical”—the direction toward the root tip of a tooth; “coronal”—the direction toward the crown of a tooth; “distal”—the direction toward the last tooth in each quadrant of a dental arch; and “mesial”—the direction toward the frontal midline in a dental arch. EDJ: enamel–dentin junction.

margins in crowns were 0.5 mm beveled, whereas the cavity margins in root were left as a butt joint. Indirect composite inlays (Grandio, Voco GmbH, Cuxhaven, Germany) were inserted without the use of an adhesive. Additionally, the inner surfaces of the inlays were polished to produce a gap between restoration and tooth [Fig. 2(a)]. The intention was to make validation reliable, as it was known that the specimens had a gap along with the entire internal interface. Three regions of interest were marked with small dots in each restoration to define reference planes through the inlays.

2.2 SS-OCT Imaging

The restorations were imaged by SS-OCT (OCS1300SS, Thorlabs Inc., New Jersey, USA, Thorlabs GmbH Dachau, Germany) [Fig. 2(b) and 2(c)]. Table 1 summarizes the specifications of the equipment. SS-OCT is a variant of Fourier domain OCT. This technique uses a tunable light source with a narrow wavelength spectrum. The axial resolution is achieved by tuning/sweeping this small spectral bandwidth through the full tunable spectral range of the light source. The detector measures the intensities of the different narrow wavelength packages sequentially as a function of time to acquire the full interference spectrum. By executing a Fourier-transform operation of the acquired signal, the determined frequencies and amplitudes give the depth information of the sample at one point. In the given approach, SS-OCT provided the combination of high imaging depth, moderate speed, and moderate resolution.

2.3 Preparation of Specimen for Histological Investigation

The specimens were embedded in Stycast® compound (Emerson & Cuming, Westerlo, Belgium) and sectioned along with the reference planes using a microtome (thickness: 200 μm , Leitz 1600 sawing-microtome, Ernst Leitz Wetzlar GmbH, Wetzlar,

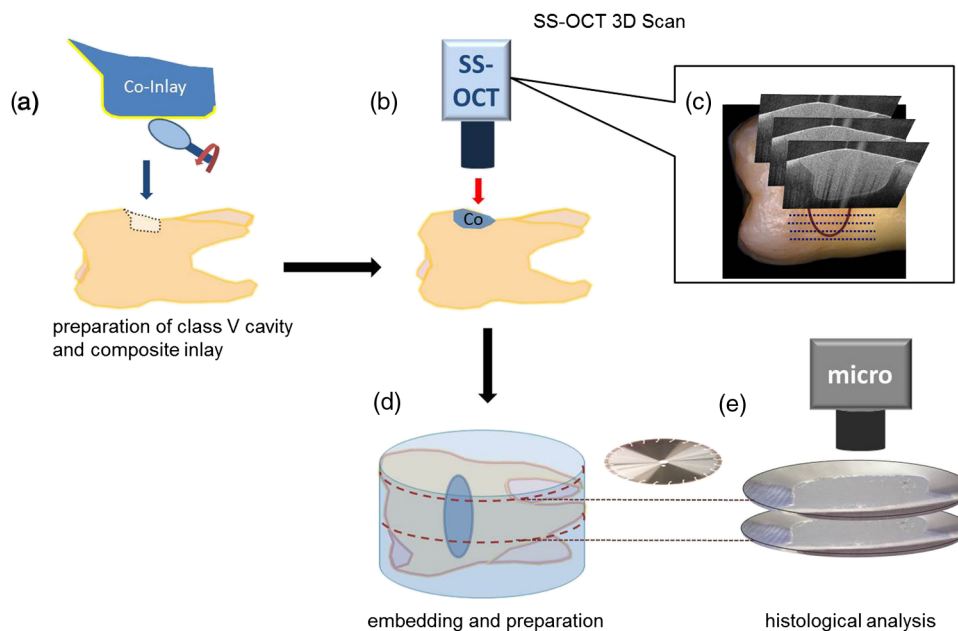


Fig. 2 Schematic depiction of the experiment. (a) Preparation of class V cavity and indirect composite inlay, polishing of the inner surface of inlay, insertion of inlay without the use of adhesive. (b) Acquisition of OCT B-scans of inlay. (c) A total of 512 B-scans in coronal-apically aligned planes (dotted blue lines) through the composite inlay were acquired. (d) Embedding of specimen and preparation of cross sections. (e) Histological analysis using light microscopy.

Table 1 Technical specification of the used SS-OCT.

Center wavelength	1325 nm
Bandwidth (3 dB)	100 nm
A-scan/line rate	16 kHz
B-scan frame rate (512 lines/frame)	25 fps
Axial (air)/lateral resolution, μm	12/25
Sensitivity	100 dB
Maximum field of view ($L \times W \times D$)	$10 \times 10 \times 3 \text{ mm}^3$
Pixel count	512×512
Power on sample	1.5 mW

Germany). Histological sections were then imaged with a light microscope (Stemi 2000-C, Carl Zeiss Microscopy GmbH, Germany) to compare with the OCT B-scans with regard to morphological properties of teeth and composite inlays [Fig. 2(d) and 2(e)].

2.4 Analysis of OCT and Histological Images

The images obtained by OCT were analyzed using ImageJ v1.45s (open source image processing and analysis in Java, Wayne Rasband, National Institutes of Health, Bethesda, Maryland, USA). A meaningful OCT signal was defined as a higher signal intensity compared to the surrounding area at the interface between tooth and composite inlay. This is in accordance with the findings of Makishi et al. who confirmed that the presence of gaps caused sharp signal growth due to reflected light at the phase boundaries of media of highly different refractive indices (i.e., air and composite).¹¹ This determination was performed visually by expert judgment as is common practice with *in vivo* imaging-based diagnostic techniques (e.g., interpretation of x-ray or ultrasound images). The OCT signal lengths were measured at the enamel-composite interfaces at the bevel and at the cavity floor-composite interfaces at dentin by means of three mesio-distally oriented B-scans per tooth. The cavity walls parallel to the laser beam were excluded from the evaluation due to there being no phase boundary in the path of the laser beam, and thus OCT producing no or unreliable signals of the gap. We defined the cavity floor—composite interfaces as being between both line angles (Line angle: junction of two surfaces of a tooth or of two walls of a tooth cavity.) of the cavity. The lengths of the gap-induced signals at the enamel margins and at the cavity floor were placed in relation to the total length of these interfaces and expressed as a percentage of total enamel margin- or floor-length, respectively (Fig. 3). Weighted average values of gap-induced signals (length, %) at enamel and dentin, respectively, were determined from 30 OCT B-scans. To determine the reproducibility of the measurement, this was repeated four consecutive times by the main observer with a minimum break of 1 week between the sessions (intra-observer analysis). Mean value as well as standard deviation and standard error of the mean (SEM) were determined.

The objectivity of the measurement was achieved by an inter-observer analysis and reproducibility was analyzed. The main observer plus three other observers (two personnel with OCT experience, one person with no prior experience in image-based diagnostics) reassessed 15 OCT B-scans randomly selected from the original set of 30 B-scans. Analogous to the intra-observer analysis, weighted average values of gap-induced signal lengths were determined by each observer. Measurements were repeated two consecutive times by each observer and mean value as well as standard deviation and standard error of the mean were determined.

Characteristics of further deficiencies in the composite restorations, such as air entrapments/large porosities or incomplete adaptation between composite increments, were also noted.

3 Results

SS-OCT B-scan images with the corresponding histological images are shown in Fig. 4. The x -axis represents the width of the scan field (512 pixels, 7 mm) and the y -axis represents the penetration depth of the OCT signals, which is dependent on the refractive index of the materials (512 pixels, up to 2.5 mm). On the OCT B-scans, the interfacial gaps between inlay and tooth showed as single or double lines with increased brightness/signal intensity. About $79.5\% \pm 1.8\%$ (SEM: 0.79) of the total gap length was detected at the enamel interface and $70.9\% \pm 0.4\%$ (SEM: 0.17) at the dentin interface. Inter-observer measurement errors of weighted means were 6.21% and 4.25% at enamel and dentin, respectively. Double lines in OCT images corresponded to gap widths of approximately $60 \mu\text{m}$ in light microscopy, whereas gap width in general ranged from 30 to $270 \mu\text{m}$ in this experimental setup.

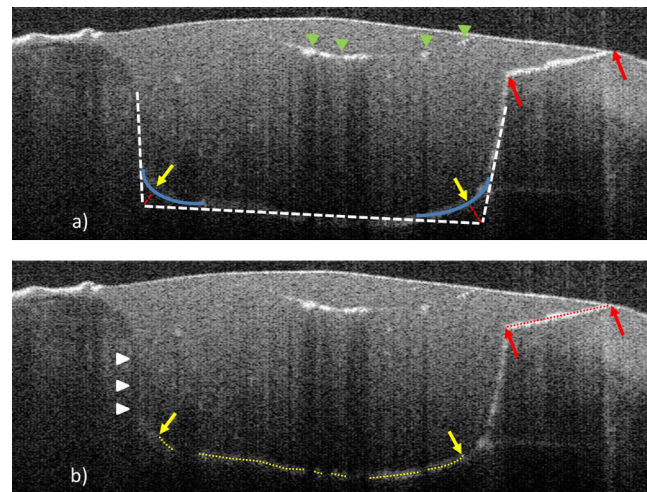


Fig. 3 OCT B-scans showing a cross section at the regions of interest. Bright lines indicate the signals for interfacial gaps. (a) The beveled enamel lies between the two red arrows while the cavity floor is between the yellow arrows. The dashed white lines indicate the extended cavity walls and floor axes. An imaginative line (dashed red lines) running from the junction of the extended axes, perpendicular to the cavity floor/wall (blue curves) defines the floor end (yellow arrows). (b) White triangles indicate the walls of the cavity which exhibit no clear signal/bright line due to their parallel orientation to the laser beam. The dotted lines indicate lengths of gap-induced OCT signals at the enamel margin (red) and at the cavity floor (yellow). Air entrapments between composite layers (asterisk), E: enamel, D: dentin, and C: composite inlay.

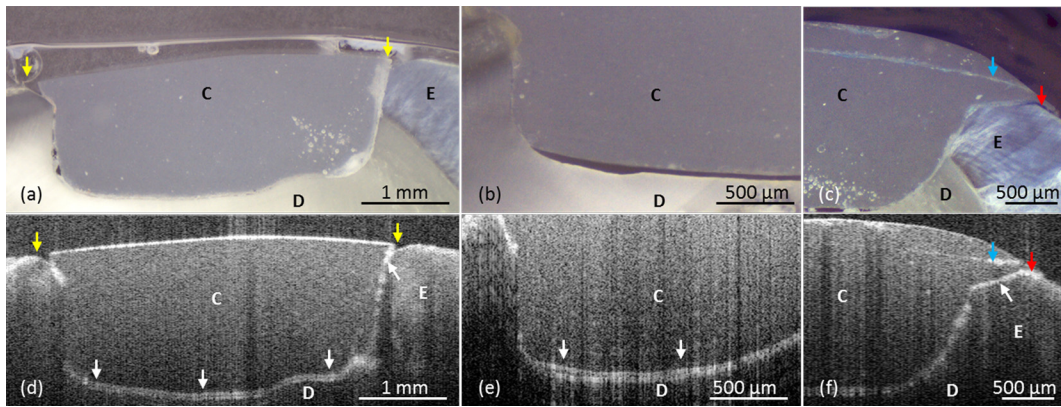


Fig. 4 OCT B-scans (d, e, and f) and light microscopic images of the corresponding cross sections (a, b, and c). Single or double line signals with high brightness indicate gaps at the composite—tooth interface (white arrows). (a and d) Yellow arrows indicate marginal gaps. (b and e) Enlargement of a section at cavity floor with structures and corresponding signals. (c and f) Enlargement of a restoration margin with excess of composite material (red arrows) and air entrapment between composite layers (blue arrows). E: enamel, D: dentin, and C: composite inlay.

OCT was able to show the enamel–dentin junction in 25 of 30 specimens [Fig. 5(a) and 5(b)]. Air entrapments or large porosities in the composite were shown as dark areas with bright outlines [Fig. 5(a) and 5(b)]. Micro-cracks in enamel and increment borders in composite layers were visible as lines of increased signal intensity [Fig. 5(c) and 5(d)].

4 Discussion

In recent years, it has been reported that OCT can be used for imaging dental tissues and dental diseases.^{12–14} These studies highlighted the potential of OCT for clinical dental application, including the diagnosis of periodontal disease and detection of carious lesions.^{12,13} It has subsequently been used *in vitro* to assess progression of carious lesions.¹⁴ Additionally, OCT has been tested as a method for investigating the integrity of dental sealants¹⁵ and tested for its ability to evaluate the adaptation of composite restorations.^{11,16} In latter studies, interfacial gaps along with the cavity were detected with great accuracy by OCT, showing the potential of the method for detecting gaps around tooth–composite restorations.^{11,16}

The suitability of OCT for gap detection is based on the large differences in refractive indices inherent to the gap area (\rightarrow phase boundaries). A gap at dental composite restorations is

characterized by a composite to air ($n_{\text{comp.}} = 1.47 - 1.56$ versus $n_{\text{air}} = 1.00$)¹⁷ and an air to enamel ($n_{\text{enamel}} = 1.63 \pm 0.007$)¹⁸ or air to dentin ($n_{\text{dentin}} = 1.54 \pm 0.013$)¹⁸ interface. This gives rise to increased light scattering and reflection and OCT signals at the gap interfaces. Our results well confirmed this by showing a probability of detection of 0.80 for interfacial defects at enamel and 0.71 at dentin. On OCT B-scans, gaps showed as single or double lines depending on gap width. Based on the manufacturer's specification which states an axial resolution of $12 \mu\text{m}$, gaps down to 24 to $36 \mu\text{m}$ (accounting for discretization) should ideally be resolved as double lines. We found that double lines on OCT B-scans represented adhesive defects with a gap width measuring $\geq 60 \mu\text{m}$. We could demonstrate this reproducibly using light microscopy.

Comparing these results with the value of 0.69 for gap detection at enamel and dentin as reported by Makishi et al. [SS-OCT data validated with confocal laser scanning microscopy (CLSM)],¹¹ it is assumed that their lower value in the comparable case without contrast agent could be due to their definition of gaps being more stringent (any interfacial spaces $>1 \mu\text{m}$ in width, as observed in CLSM images) and clearly below the expected resolution of OCT, thus lowering sensitivity. Moreover, artificial interfacial defects probably introduced

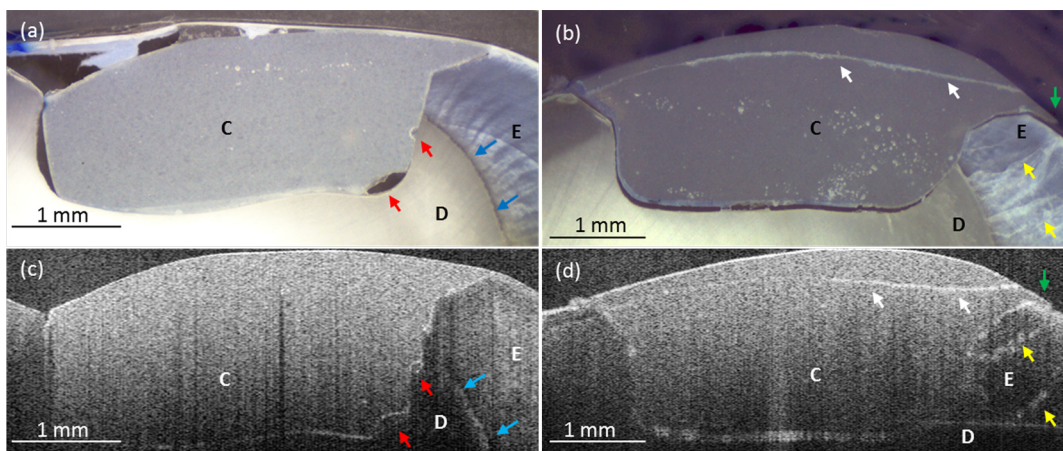


Fig. 5 OCT B-scans (c and d) with corresponding optical microscopic images (a and b). Air entrapments (red arrows), enamel–dentin junction (blue arrows), micro-cracks in enamel (yellow arrows), increment borders of the composite layers (white arrows), excess of composite material (green arrows). E: enamel, D: dentin, and C: composite inlay.

during specimen preparation was a differentiating factor to our studies probably having led to greater gap lengths observed by CLSM.

It is noted, although, that with our approach we were not able to determine the rate of false positive diagnoses due to the absence of gap-free interfaces. This will have to be determined in subsequent studies before OCT's ability to reliably detect gaps can be conclusively proven.

To our knowledge, no other nondestructive diagnostic methods suited for gap detection and assessment along with the cavity walls and cavity floors have been systematically assessed. Therefore, we cannot directly compare our findings with other data. For a general comparison, sensitivities of established dental methods for other areas of caries detection are presented for informational purposes:¹⁹

- Visual detection of primary caries depending on surface and extent: 37% to 66%.
- X-ray: 30% to 73%.
- Laser fluorescence (DIAGNOdent): 72% to 78%.

Compared to these techniques, the detection rate of OCT in our study is on a high level. We noted that air entrapments/large porosities in the composite layers caused significant OCT signal loss, impairing the probability to detect interfacial gaps underneath (Fig. 3). However, we predict more reliable detection of gaps when beaming direction is varied during imaging to circumvent shading effects. Moreover the detection of air entrapments, porosities, and composite increment borders could be of additional benefit, because these defects are currently not clinically detectable and are potential weak spots of restorations. Thus, OCT will help assuring quality of restorative procedures and results both during and after placement.

Other limitations of OCT that we encountered during our study were that structures located parallel to the laser beam were not visible. This problem can also again be overcome by varying the projection axis of the laser beam. Another phenomenon noted was that the image scale in the vertical-/depth direction of OCT images varies depending on the refractive index of the different materials.

The equipment used enabled us to confirm that SS-OCT has an average penetration depth of up to 2.5 mm in dental hard tooth tissues. With an enamel thickness of up to 2.5 mm, this is generally sufficient to display the EDJ and adjacent dentin structures. It is assumed that in clinical practice, penetration depth and resolution will also be influenced by additional factors such as plaque, stain or calculus on the tooth surface, and hydration. These phenomena represent additional face boundaries, therefore cleaning and air drying of the tooth surface is expected to be necessary to achieve best performance.

The results of this study demonstrate the potential of OCT imaging to nondestructively and noninvasively detect and assess defects between hard tooth tissues and composite restorations, and to discover imperfections within the layered composite. Our results indicate that OCT could provide additional diagnostic information in single and longitudinal assessments of composite restoration. This technique offers the potential to longitudinally

assess these restorations chair-side and to estimate whether detected defects are stable or changing.

Acknowledgments

Thorlabs GmbH, Dachau, Germany for provision of the OCT equipment, Timothy Jones (IALT, University of Leipzig, Germany) for editorial assistance and Ms. Rueger for the professional technical assistance.

References

1. F. Lutz, I. Krejci, and F. Barbakow "Quality and durability of marginal adaptation in bonded composite restorations," *Dent. Mater.* **7**(2), 107–113 (1991).
2. N. J. Opdam, F. J. Roeters, and E. H. Verdonchot "Adaptation and radiographic evaluation of four adhesive systems," *J. Dent.* **25**(5), 391–397 (1997).
3. I. A. Mjör "The reasons for replacement and the age of failed restorations in general dental practice," *Acta Odontol. Scand.* **55**(1), 58–63 (1997).
4. E. A. Kidd "Caries diagnosis within restored teeth," *Adv. Dent. Res.* **4**(1), 10–13 (1990).
5. R. Haak et al., "Detection of marginal defects of composite restorations with conventional and digital radiographs," *Eur. J. Oral Sci.* **110**(4), 282–286 (2002).
6. D. Huang et al., "Optical coherence tomography," *Science* **254**(5035), 1178–1181 (1991).
7. A. G. Podoleanu "Optical coherence tomography," *Br. J. Radiol.* **78**(935), 976–988 (2005).
8. B. Liu and M. E. Brezinski "Theoretical and practical considerations on detection performance of time domain, Fourier domain, and swept source optical coherence tomography," *J. Biomed. Opt.* **12**(4), 044007 (2007).
9. A. F. Fercher "Optical coherence tomography—development, principles, applications," *Z. Med. Phys.* **20**(4), 251–276 (2010).
10. J. G. Fujimoto et al., "Optical coherence tomography: an emerging technology for biomedical imaging and optical biopsy," *Neoplasia* **2**(1–2), 9–25 (2000).
11. P. Makishi et al., "Non-destructive 3D imaging of composite restorations using optical coherence tomography: marginal adaptation of self-etch adhesives," *J. Dent.* **39**(4), 316–325 (2011).
12. B. Colston et al., "Dental OCT," *Opt. Express* **3**(6), 230–238 (1998).
13. D. P. Popescu et al., "Assessment of early demineralization in teeth using the signal attenuation in optical coherence tomography images," *J. Biomed. Opt.* **13**(5), 054053 (2008).
14. D. Fried et al., "Imaging caries lesions and lesion progression with polarization sensitive optical coherence tomography," *J. Biomed. Opt.* **7**(4), 618–627 (2002).
15. A. K. Braz, C. M. Aguiar, and A. S. Gomes "Evaluation of the integrity of dental sealants by optical coherence tomography," *Dent. Mater.* **27**(4), e60–e64 (2011).
16. T. A. Bakhsh et al., "Non-invasive quantification of resin–dentin interfacial gaps using optical coherence tomography: validation against confocal microscopy," *Dent. Mater.* **27**(9), 915–925 (2011).
17. A. C. Shortall, W. M. Palin, and P. Burtscher "Refractive index mismatch and monomer reactivity influence composite curing depth," *J. Dent. Res.* **87**(1), 84–88 (2008).
18. Z. Meng et al., "Measurement of the refractive index of human teeth by optical coherence tomography," *J. Biomed. Opt.* **14**(3), 034010 (2009).
19. J. D. Bader, D. A. Shugars, and A. J. Bonito "Systematic reviews of selected dental caries diagnostic and management methods," *J. Dent. Educ.* **65**(10), 960–968 (2001).